International Journal of Engineering

Journal Homepage: www.ije.ir

New Approach of Deployment of the Multi-static Radars Based on an Aperture Angle and the Probability of False Alarm

I. E. Luc*[a], E. D. Jean-François[a,b,c], M. Jacques[b], Y. S. Joe[d]

[a] *Technology and Applied Sciences Laboratory, University Institute of Technology of Douala, University of Douala, Douala, Cameroon*
[b] *Laboratory of Energy, Materials, Modeling and Methods, National Higher Polytechnic School of Douala, University of Douala, Douala, Cameroon*
[c] *Department of Electrical Engineering, Advanced Teachers' Training College for Technical Education, University of Douala, Douala, Cameroon*
[d] *Department of Physics and Astronomy, Ball State University, Muncie, IN 47306, USA*

PAPER INFO

Paper history:
Received 31 March 2023
Received in revised form 09 May 2023:
Accepted 24 May 2023

Keywords:
Aperture Angle
Probability of False Alarm
Multi-static Radar
Sensor Spacing
Tomographic Resolution

ABSTRACT

This article proposes a new engineering approach to detect targets using multi-static radars. It considers the aperture angle and the probability of false alarm of detection which allow to improve the performances of the radar system deployment. This proposed method is tested on three tomographic modes of multi-static radars: Single Input Multiple Output (SIMO), Multiple Input Multiple Output (MIMO), and Synthetic Aperture Radar (SAR). In this work, a calculation and estimation method for the parameters (spacing sensor and tilt angle of baseline) are developed using the deployment of the radar system based on geometrical arrangements. Employing these parameters, estimated by the proposed approach, and using them for the calculation of the tomographic resolution, the nearest ambiguity location, and the scan loss which are radar deployment performances. The results show that the spacing between sensors varies from 40 to 70% with an increment of aperture angle from 15° to 30° and the step of 10^{-3} variation in the false alarm probability of detection. The length of the radar system deployment is also reduced by 6.66%. This approach improves the capabilities of distinction of the targets in a multi-static radar system and allows a reduction in deployment costs.

***doi**: 10.5829/ije.2023.36.09c.01*

1. INTRODUCTION

The range resolution can be enhanced by decreasing the bandwidth, which depends on the transmit array geometry. The achievable resolution of the estimation direction depends on the receive array geometry [1]. Multi-static radars studies formed into array created several works based on the estimation methods of the arrived angles of signals (by coupling them with the types of the sensor's radars) [2-6], the geometrical form of deployment of these sensors [7, 8], and the slope angle of the radiation pattern [9, 10]. It is the case introduced by Shen and Wang [7], which they have used planar geometry in order to solve the problem of extraction of poles in 2-D. The circular geometry coupled with the Bayesian method [8] and a linear geometry formed of monostatic radars [2, 3] are used in considering the arrived angles of signals.

Nowadays, the improvement of the performance of a radar system is based on the algorithms for the targets detection and on the deployment environments [11-13]. There are several parameters which allow to evaluate the performances emanating from the radar equation [14]. The performance can also be analyzed according to technologies which are characteristic of the nature of the used signals for the transmitters [15]. Thus, criteria such as resolution can be used to determine the ability of a radar to identify several distinct targets [16] and the location of the nearest ambiguity can be used to determine how far away the radar can detect the next ambiguity or replica [17]. In addition to these parameters, we also have the probability of detection which is the possibility that a radar receives the echo of a target compared to the noise [18, 19]. All the multi-static radar systems have parameters of deployment such as spacing between the sensors, the physical angle of slope, the slope

*Corresponding Author Email: eyembeluc@yahoo.fr (I. E. Luc)

Please cite this article as: I. E. Luc, E. D. Jean-François, M. Jacques, Y. S. Joe, New Approach of Deployment of the Multi-static Radars Based on an Aperture Angle and the Probability of False Alarm, ***International Journal of Engineering, Transactions C: Aspects***, Vol. 36, No. 09, (2023), 1589-1596

compared to the base line, and the number of sensor's radars for the formation of the array [17]. Multi-static radars is primarily formed of phased antenna arrays [20-23] and spacing between them is estimated in wavelength [24]. This method works well for small-scale deployments at large frequencies, requiring small antennas [19, 25, 26]. However, for large-scale deployments, such as satellite radar platforms, it is difficult to determine the wavelength spacing [27]. Moreover, development of consumer loyalty of the sensors decreases the fidelity of the simulated scene as well as the complexity of the formation geometry, which is a problem.

This paper aims to target detection in multi-static radars which mainly focus on the specific interesting area. The approach used consider the aperture angle and the probability of false alarm detection in order to improve the performance of the radar system such as tomographic resolution, location of the nearest ambiguity, and scanning losses.

This article is organised as follows: The first section is based on the introduction. Second section explains the problem, materials technique, along with some working assumptions, and a suggested solution is offered. Section 3 presents the findings and related discussion. Conclusions are provided in section 4.

2. MATERIALS METHOD

2. 1. Problem Description Let us consider an imagery tomographic system for multi-static radar represented in Figure 1. The system is placed in space up to altitude H and is composed of N identical sensors radars having a regular spacing d and deployed on the $N \times d$ distance. θ represents the angle of sight compared to the ground, Ω is the aperture angle of the sensor radar, ε is the tilt angle compared to the base line and D is the range of the radar following the r direction. The geometry of deployment in Figure 1 admits a symmetry at the level of the placement of the sensor's radars. The radar's sensors are assumed to be distributed along a line in the across-track plane and can transmit and receive or be received-only depending on the tomographic mode (SIMO, SAR and MIMO). The quality of 2-D tomographic images on the ground-range (vertical and horizontal) plane depends on the tomographic performance along the look direction r and along n (perpendicular to look direction), which are coupled via the angle of sight and the local terrain slope μ. Therefore, in addition to resolution and ambiguity along n, ambiguity along r and range resolution were also included. The resolution in distance is a function of the bandwidth of transmission and it is expressed in Equation (1):

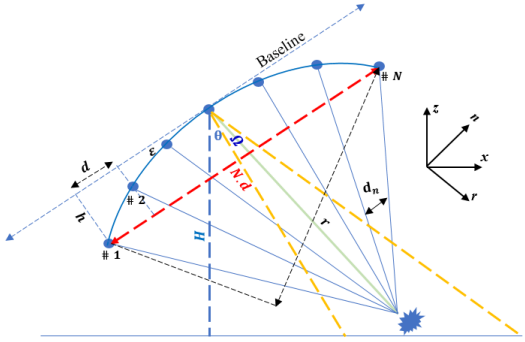

Figure 1. Multi-static observation geometry, relevant parameters, and spatial directions

$$\delta_r = \omega_r \frac{c}{2B} \quad (1)$$

where c is the speed of the light in the vacuum, B is the bandwidth of the transmitted signal, and ω_r is the coefficient of expansion applied to reduce the side lobes by considering the effects of fenestration.

The performances of the multi-static radars depend on two parameters: the spacing between the sensors and the tomographic resolution along the normal direction (n) in the plane, which depends on the maximum length of the basic deployment. Its equation is similar to the equation of resolution of the SAR, the synthetic aperture length replaced by the basic tomographic deployment length δ_n:

$$\delta_n = \omega_n \frac{\lambda D}{\rho_n L_n} \quad (2)$$

where λ is the wavelength, $D = \frac{H}{cos\theta}$ is the range of the sensor radars which is the center of symmetry of the architecture, $L_n = N \cdot d \cdot \cos(|\theta - \omega|)$ is the per-pendicular maximum length of the base line $\omega_n = \omega_r$.

While replacing L_n in the expression (2), we obtained:

$$\delta_n = \frac{\omega_n}{p_\delta} \frac{\lambda H}{N \cdot d \cdot \cos(|\theta - \omega|) \cos\theta} \quad (3)$$

where p_δ is the coefficient of resolution depending on the multi-static mode.

Platform spacing that is periodic leads to ambiguous returns, often known as target replicas [28, 29]. The closest (relative to the real target) ambiguity's position is crucial since it helps define how much of the target may be photographed without copies overlapping. It should be noted that ambiguous copies of targets outside the scene of interest might nonetheless fall within the scene of interest, even if the scene of interest is smaller than the position of the nearest ambiguity. The closest ambiguity for a flat surface, according to Seker and Lavalle [17], is at:

$$A_n^1 = \pm \frac{\lambda H}{p_a d_n \cos\theta} \quad (4)$$

where p_a is the coefficient of localization of an ambiguity and $d_n = dcos(|\theta - \omega|)$.

Here, the spacing d between sensor's radars is generally determined by deployments requiring large spacings such as satellites by:

$$dx = \frac{2*v*PRI}{\psi} \quad (5)$$

where v is the orbital velocity, PRI is the pulse repetition interval and ψ is a factor to reduce the pulse repetition rate. The systems, which use Equation (5) to make the deployment, encounter the problem of radar fidelity on the area of interest involving noise due to the signals of the replicas.

2. 2. Proposed Solution To solve the radar retention problem in the target area, the probability of false detection alarm and the aperture angle on radar system were used. The probability α of false alarm is defined as the probability that a sample of the signal $r(t)$ will exceed the threshold of tension V_T when the noise alone is present in the radar:

$$\alpha = \int_{V_T}^{\infty} \frac{r}{\sigma^2} exp\left(-\frac{r^2}{2\sigma^2}\right) dr = exp\left(\frac{V_T^2}{2\sigma^2}\right) \quad (6)$$

where $V_T = \sqrt{2\sigma^2 \, ln\left(\frac{1}{\alpha}\right)}$ and σ is the variance.

Figure 2 shows the evolution of the probability of detection according to the signal to noise ratio (SNR) under several values of the probability of false alarm. We observe that the probability of false alarm influences the capacity of a receiver radar in the sense that as α becomes small, the ratio signal to noise increases. This also effected on the parameters of deployment and the performances.

In the case of antennae having only one beam, the aperture angle of the beam represents the solid angle through which all the power radiated by the antenna is concentrated.This aperture angle of the beam, Ω_a, is given by:

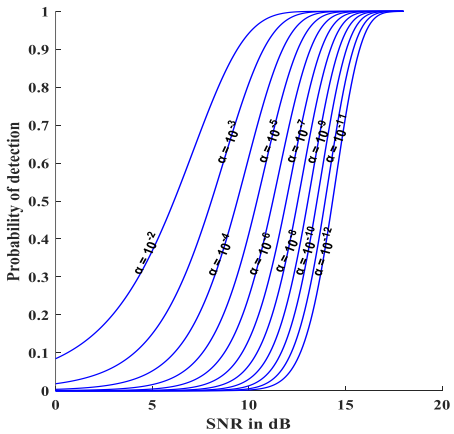

Figure 2. Probability of detection

$$\Omega_a = \oint K_n(\theta, \phi) \, d\Omega. \quad (7)$$

The probability of false alarm detection and the aperture angle of a radar are used to determine the spacing between the radars as follows.

Let us consider a multi-static system formed of N aligned sensors radars and the aperture angle Ω as illustrated in Figure 3. By considering the triangles (OEB) and (OAB), we can express $\cos(\Omega/2)$ in the form as $\cos(\Omega/2) = OB/OE$ and $\cos(\Omega/2) = OA/OB$, respectively.

By multiplying the two values, we obtained:

$$cos^2\left(\frac{\Omega}{2}\right) = \frac{OA}{OE} \quad (8)$$

where $OA = OE \cos^2\left(\frac{\Omega}{2}\right)$ and $OE = \alpha D$. In the triangle (OAB), we have $d = OA \tan\left(\frac{\Omega}{2}\right)$ with $AB = d$. Now, we obtained a regular spacing d between the sensors as follows:

$$d = \alpha D \cos\left(\frac{\Omega}{2}\right) \sin\left(\frac{\Omega}{2}\right) \quad (9)$$

In our case, we proposed to use an elliptic architecture (Figure 1) having the length of the semi-major and semi-minor axes a and b: $a = \frac{N.d}{2}$ and $b = h$, where $h < \frac{N.d}{2}$.

In this architecture, we have an angle of the curve ε which is formed between the baseline and symmetrical elliptic architecture. This angle can be expressed in the form:

$$\varepsilon = \tan^{-1}\left(\frac{2h}{d(N-1)}\right) \quad (10)$$

By replacing d by its equation (10), we have:

$$\varepsilon = \tan^{-1}\left(\frac{2h}{(N-1)\alpha D \cos\left(\frac{\Omega}{2}\right)\sin\left(\frac{\Omega}{2}\right)}\right) \quad (11)$$

Here, ε represents necessary calibration to better deploy a satellite radar system on the basis of the principle that the ground has an elliptic form. For primarily reasons related to the practice, it is necessary that $h \leq \alpha D$. In the tomographic radars the formation of

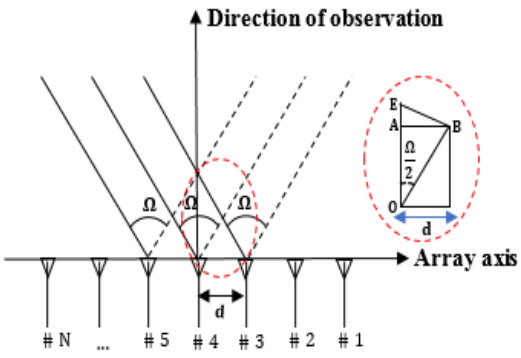

Figure 3. Geometry for calculation of spacing

the spotlight is very significant; this is why the designers find the compromise between the adequate spacing of the sensors radars in term of the value of d and the angle slope compared to the normal of the direction of observation φ. We can thus determine φ by the following relation:

$$\varphi = \frac{\pi}{N-1} \tag{12}$$

Equation (3) presents the parameters entering the determination of the tomographic resolution without considering the probability of a false alarm and the aperture angle. Thus, we propose to insert d of Equation (9) into Equation (3), we obtained then:

$$\delta_n = \frac{\omega_n}{p_\delta} \frac{\lambda}{\alpha \cos\left(\frac{\Omega}{2}\right) \sin\left(\frac{\Omega}{2}\right) N \cos\left(|\theta-\omega|\right)} \tag{13}$$

Equation (13) allows to focus on the zone delimited by the aperture angle of the sensor radar to avoid having information about the not targeted zones which are sources of perturbations.

Equation (4) does not integrate the aperture angle and the probability of false alarm and the probability of having replicas which are not in the zone of interest. While substituting Equation (9) into Equation (4), the nearest ambiguity with the aperture angle and the probability of false alarm is obtained by:

$$A_n^1 = \pm \frac{\lambda}{p_a \alpha \cos\left(\frac{\Omega}{2}\right) \sin\left(\frac{\Omega}{2}\right) \cos(|\theta-\omega|)} \tag{14}$$

3. RESULTS AND DISCUSSION

Figure 4 represents the evolution of spacing between the sensors as a function of the range of the radar (up to 800 km) for four values of the probability of false alarm of the detection of order 10^{-3} under three different apertures angles. The numerical results show that the spacing between the sensors varies when both the probability of false alarm detection and the apertures angle changes.

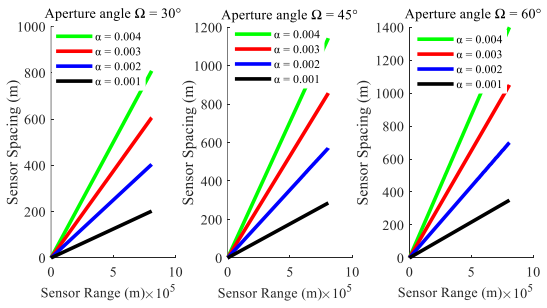

Figure 4. Evolution of spacing between the sensor's vs radar sensor range for four values of the probability of false alarm detection under three different apertures angles

Note that variations of spacing between the probabilities of false alarm are 200 m for $\Omega = 30°$, 285 m for $\Omega = 45°$, and 350 m for $\Omega = 60°$, respectively.

When the probability of false alarm detection becomes extremely small for a fixed apertures angle, this variability of spacing is decreasing. The percentage in the increase of spacing radar sensor vs. the probability of false alarm detection under three apertures angles is shown in Figure 5. When the aperture angle of reference is taken as $\Omega = 30°$, an increase in average distance for the tested values of α is about 41% as Ω varies from 30° to 60° and 73% as Ω varies from 30° to 60°.

The tilted angle of the base line as a function of the spacing of the sensor's radars is presented in Figure 6 for four different probabilities of false alarm (detection of order 10^{-3} under three different apertures angles). This angle, used in Equation (12), is the angular variation of the normal (r direction) towards the base line.

Note that the angle of inclination of the baseline decreases when the aperture angle increases and the probability of false alarm increases. We find that the variations in angle between the probabilities of false alarm is 7° for $\Omega = 30°$, 9° for $\Omega = 45°$, and 10° for $\Omega = 60°$. Figure 7 presents the percentage decrease in the tilted baseline angle vs the probability of false alarm using the same parameters Figure 6. Percentage of

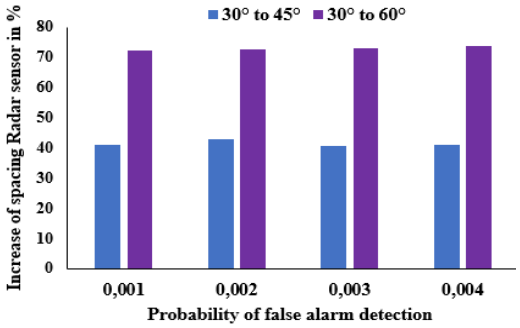

Figure 5. Percentage in the increase of spacing radar sensor vs. the probability of false alarm detection under three apertures angles

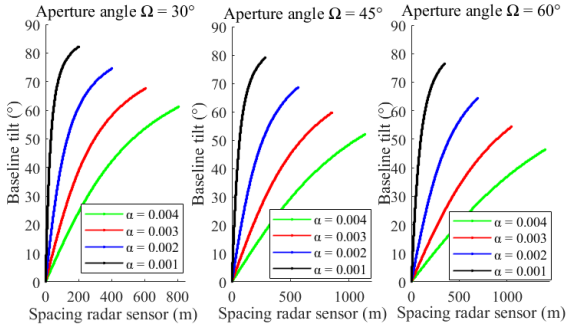

Figure 6. Evolution of the tilted angle of the baseline vs. the spacing of the sensor's radars

increase in spacing radar sensor vs. the probability of false alarm detection under three apertures angles in Figure 7. Observe that with a reference of the aperture angle $\Omega = 30°$, the percentage in the angle of inclination of the base line decreases according to the decrease of α and the growth of Ω.

Figure 8 presents the tomographic resolution with a bilateral resolution of 4 dB under various multi-static modes of radars. In the two left figures of Figure 8, three dashed lines are obtained with parameter values of $\theta = 30°, \varepsilon = 30°$ (Figure 8(a)) and $\theta = 60°, \varepsilon = 60°$ (Figure 8(b)) [17].

In the meantime, we add the aperture angle $\Omega = 30°$ (Figure 8(a)) and $\Omega = 60°$ (Figure 8(b)) and obtain the tomographic resolution for three multi-static modes (three solid lines). In the two right figures of Figrue 9, it is exactly the same situation as the two left ones of Figure 9 except that we have different values of the tilted angle of the baseline, $\varepsilon = 60°$ (Figure 8(a)) and $\varepsilon = 45°$ (Figure 8(b)).

We obtained a spacing between radars d=1400 m using our approach, whereas d=1500 m is used by Seker and Lavalle [17]. We note here that when $\theta = 30°$, $\varepsilon = 30°$ or $\theta = 60°$, $\varepsilon = 60°$, the resolution is the same even if we include the aperture angle in our calculation (two

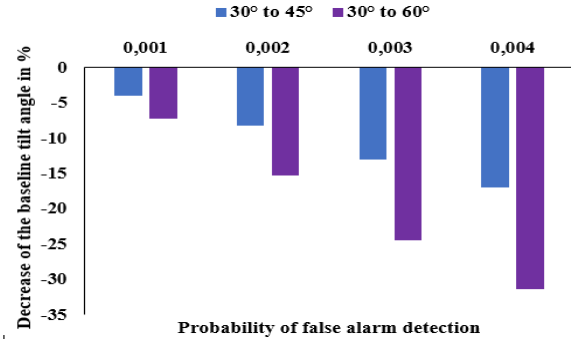

Figure 7. Percentage in the tilted angle of the baseline vs. the probability of false alarm of detection under three apertures angles

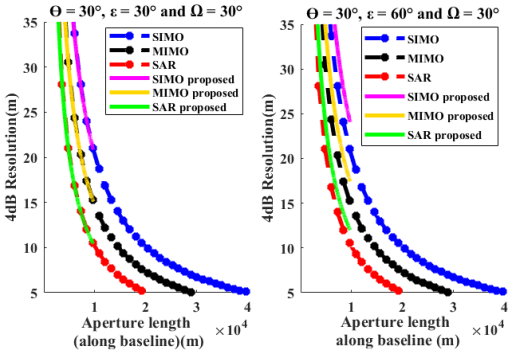

(a)

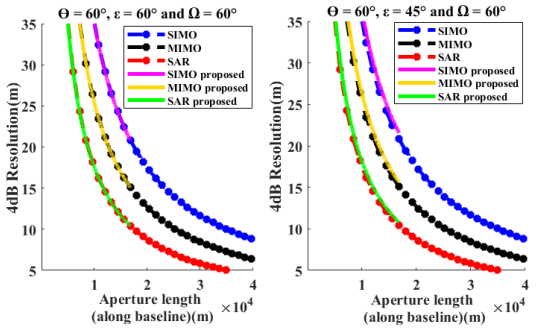

(b)

Figure 8. Tomographic resolution vs. aperture length for look angle: (a) θ = 30° and (b) θ = 60°

left figures of Figure 9). When we consider $\varepsilon = 60°$the aperture angle $\Omega = 60°$ with $\theta = 60°$, $\varepsilon = 45°$, however, we obtained a resolution increase of 1.84 m in mode SIMO, of 1.6 m in mode MIMO, and of 1.05 m in mode SAR for an aperture length of 10 km. (right figure of Figure 9(b)). In the case of $\Omega = 30°$ with $\theta = 30°$, , we have a resolution increase of 5.14 m in mode SIMO, of 3.52m in mode MIMO, and of 2.58 m in mode SAR when a length of aperture is 10 km (right figure of Figure 8 (a)).

The localization of the nearest ambiguity as a function of the spacing to sensor's radars for a probability of false alarm of detection $\alpha = 4 \times 10^{-3}$ is shown in Figure 10. Here, Figure 9(a) is obtained with the same parameters as reported by Seker and Lavalle [17] and Figure 9(b) presents the localization of nearest ambiguity while applying Equations (3) and (14). It is interesting to note that we have the same results when we changed the basic angle of slope. We obtained a better localization of the zone of interest by taking into account the aperture angle and the probability of false alarm detection in the determination of the localization of the nearest ambiguity corresponding to the selected spacing. This allows to fight against the problem of the replicas that we meet out of tomographic radars.

Figure 10 represents the amplitude of the power reflected by the target and received by the receivers for the SIMO, MIMO, and SAR modes. Observe that the amplitude peaks reproduce in a specific distance to the SIMO, MIMO and SAR corresponding to the resolution estimated in left-side of Figure 8(b). The system in SIMO mode detects two separate targets at 10 m and 20 m while the two others are at 15 m and 21 m, respectively.

We noted a maximum level of sidelobe is -15 dB in the MIMO and SAR system and -10 dB in the SIMO system. The effects of the aperture angle and the probability of false alarm of detection allow to improve the precision of the parameter values in the multi-static radar system.

Table 1 compares the values for Theoretical Resolution 4dB (TR4dB), Theoretical Ambiguity

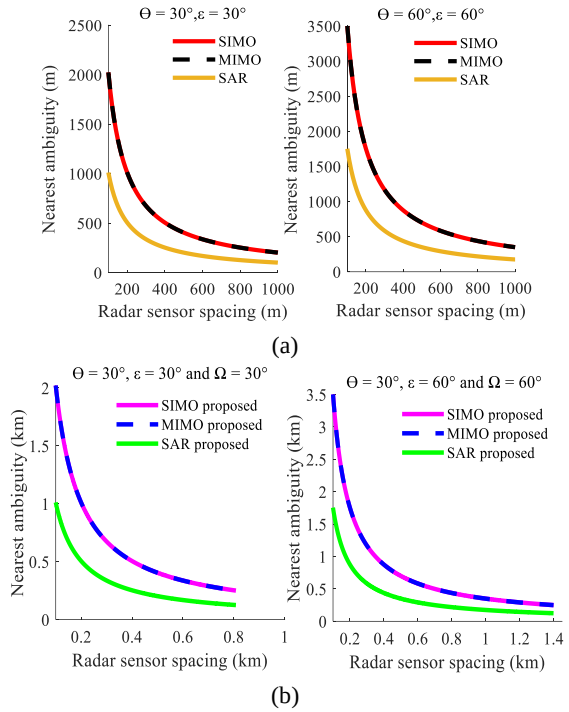

Figure 9. Nearest ambiguity location vs. platform spacing for two different cases, (a) as per [17] and (b) as per Equation (14)

Location (TAL), and Maximum Sidelobe Level (MLS). This comparison is done between the suggested approach and that presented in the literature [17]. The suggested method is less effective in the 4dB resolution than [17], and this is also true for the sidelobe level.

This approach improves the literature in terms of ambiguity location and enables, through the introduction of the false alarm probability and the aperture angle, to have a spacing that allows for the achievement of a high signal-to-noise ratio, thereby limiting the impact of the replicas that raise the noise level and lower the detection capability of two targets when they are close to one another.

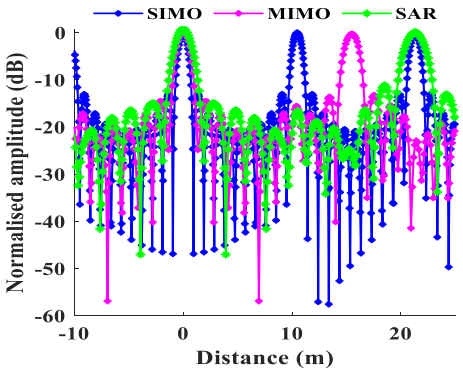

Figure 10. Tomographic "images" in 1-D for the SAR, SIMO, and MIMO modes

TABLE 1. Comparison of results

	Ref. [17]			**Proposed approach**		
	Spacing = 1500 m			Spacing = 1400		
	SAR	SIMO	MIMO	SAR	SIMO	MIMO
TR 4dB	4.9 m	9.7 m	7.0 m	6.5 m	13 m	9.5 m
TAL	58 m	117 m	117 m	10 m	15 m	21 m
MLS	-13 dB	-13 dB	-26 dB	-13 dB	-13 dB	-15 dB

4. CONCLUSION

In conclusion, we have considered the aperture angle and the probability of false alarm detection in the estimation of the parameters of deployment in order to improve the multi-static performances of the radars. This new approach has allowed to develop an estimation method for the spacing between the sensor's radars for deployments on a large scale and the angle of slope of the baseline. The performance evaluations with the aperture angle and the probability of false alarm of detection such as the resolution, the ambiguity and the scan loss have been examined. We also determined the physical angle of slope allowing the sensor's radars to form a spotlight. Our approach was tested under three multi-static modes of radars. The results showed that the multi-static performances of the radars, like their deployment, were improved. In addition, it solves the problems related to the complexity of the deployment geometries in the multi-static radar systems. In particular, the SAR, which has realistic values of resolution, locates on the area covered by the spotlight formed by several sensors in order to avoid noise due to areas of no interest.

Future research on the optimal estimation of the tilt angle of the baseline and the aperture angle to make a better compromise to reduce the losses of scanning and to make an experimental study by applying our approach will be necessary.

5. REFERENCES

1. Hyder, M.M., Mahata, K. and Hasan, S.M., "A new target localization method for bistatic fda radar", ***Digital Signal Processing***, Vol. 108, (2021), 102902. doi: 10.1016/j.dsp.2020.102902.
2. Li, Z. and Zhang, X., "Monostatic mimo radar with nested l-shaped array: Configuration design, dof and doa estimation", ***Digital Signal Processing***, Vol. 108, (2021), 102883. doi: 10.1016/j.dsp.2020.102883.
3. Wen, F., Mao, C. and Zhang, G., "Direction finding in mimo radar with large antenna arrays and nonorthogonal waveforms", ***Digital Signal Processing***, Vol. 94, (2019), 75-83. doi: 10.1016/j.dsp.2019.06.008.
4. Jia, Y., Chen, C., Zhong, X., Yan, C., Duo, B. and Guo, Y., "Doa estimation of coherent and incoherent targets based on monostatic co-prime mimo array", ***Digital Signal Processing***, Vol. 94, (2019), 56-66. doi: 10.1016/j.dsp.2019.06.004.

5. Tian, Y., Lian, Q. and Xu, H., "Mixed near-field and far-field source localization utilizing symmetric nested array", ***Digital Signal Processing***, Vol. 73, (2018), 16-23. doi: 10.1016/j.dsp.2017.10.021.
6. Huang, Y., Liao, G., Li, J., Li, J. and Wang, H., "Sum and difference coarray based mimo radar array optimization with its application for doa estimation", ***Multidimensional Systems and Signal Processing***, Vol. 28, (2017), 1183-1202. doi: 10.1007/s11045-016-0387-2.
7. Shen, H. and Wang, B., "Two-dimensional unitary matrix pencil method for synthesizing sparse planar arrays", ***Digital Signal Processing***, Vol. 73, (2018), 40-46. doi: 10.1016/j.dsp.2017.10.019.
8. Behmandpoor, P. and Haddadi, F., "Circular array design based on bayesian cramer–rao bound", ***Multidimensional Systems and Signal Processing***, Vol. 31, (2020), 317-328. doi: 10.1007/s11045-019-00668-1.
9. Wang, W., Ren, S. and Chen, Z., "Unified coprime array with multi-period subarrays for direction-of-arrival estimation", ***Digital Signal Processing***, Vol. 74, (2018), 30-42. doi: 10.1016/j.dsp.2017.11.015.
10. Wang, W., Zhang, Q., Tan, W., Shi, W. and Pang, F., "Direction finding via acoustic vector sensor array with non-orthogonal factors", ***Digital Signal Processing***, Vol. 108, (2021), 102910. doi: 10.1016/j.dsp.2020.102910.
11. Ahmad, F. and Amin, M.G., "A noncoherent approach to radar localization through unknown walls", in 2006 IEEE Conference on Radar, IEEE. (2006).
12. Rabe, H., Denicke, E., Armbrecht, G., Musch, T. and Rolfes, I., "Considerations on radar localization in multi-target environments", ***Advances in Radio Science***, Vol. 7, (2009), 5-10. doi: 10.5194/ars-7-5-2009.
13. Schreiber, R. and Bajer, J., "Time difference measurement algorithm for tdoa positioning system using rtl-sdr", in 2017 International Conference on Military Technologies (ICMT), IEEE. (2017), 608-612.
14. George, B.A., Obot, A.B. and Udofia, K.M., "Modelling and performance evaluation of ground based monostatic radar surveillance system", ***Communications***, Vol. 7, (2019), 17-21.
15. Yang, J., Qiu, Z.-K., Li, X. and Zhuang, Z.-W., "Uncertain chaotic behaviours of chaotic-based frequency-and phase-modulated signals", ***IET Signal Processing***, Vol. 5, No. 8, (2011), 748-756. doi: 10.1049/iet-spr.2010.0096.
16. Grasso, M., Renga, A., Fasano, G., Graziano, M., Grassi, M. and Moccia, A., "Design of an end-to-end demonstration mission of a formation-flying synthetic aperture radar (ff-sar) based on microsatellites", ***Advances in Space Research***, Vol. 67, No. 11, (2021), 3909-3923. doi: 10.1016/j.asr.2020.05.051.
17. Seker, I. and Lavalle, M., "Tomographic performance of multi-static radar formations: Theory and simulations", ***Remote Sensing***, Vol. 13, No. 4, (2021), 737. doi: 10.3390/rs13040737.
18. Zaimbashi, A. and Li, J., "Tunable adaptive target detection with kernels in colocated mimo radar", ***IEEE Transactions on Signal Processing***, Vol. 68, (2020), 1500-1514. doi: 10.1109/TSP.2020.2975371.
19. Golbon-Haghighi, M.-H., Mirmozafari, M., Saeidi-Manesh, H. and Zhang, G., "Design of a cylindrical crossed dipole phased array antenna for weather surveillance radars", ***IEEE Open Journal of Antennas and Propagation***, Vol. 2, (2021), 402-411. doi: 10.1109/OJAP.2021.3059471.
20. Fenn, A.J., Temme, D.H., Delaney, W.P. and Courtney, W.E., "The development of phased-array radar technology", ***Lincoln Laboratory Journal***, Vol. 12, No. 2, (2000), 321-340.
21. Basit, A., Khan, W., Khan, S. and Qureshi, I.M., "Development of frequency diverse array radar technology: A review", ***IET Radar, Sonar & Navigation***, Vol. 12, No. 2, (2018), 165-175. doi: 10.1049/iet-rsn.2017.0207.
22. Jeon, S.-I., Kim, Y.-W. and Oh, D.-G., "A new active phased array antenna for mobile direct broadcasting satellite reception", ***IEEE Transactions on Broadcasting***, Vol. 46, No. 1, (2000), 34-40. doi: 10.1109/11.845863.
23. Wei, Y., Zhang, X., Bai, Y. and Tang, L., "A novel range alignment method for isar based on linear t/r array model", ***Multidimensional Systems and Signal Processing***, Vol. 25, No. 4, (2014), 759-773. doi: 10.1007/s11045-013-0229-4.
24. Mahafza, B.R., "Radar signal analysis and processing using matlab, CRC Press, (2016).
25. Sridher, T., Sarma, A. and Naveen Kumar, P., "Performance evaluation of onboard wi-fi module antennas in terms of orientation and position for iot applications", ***International Journal of Engineering, Transactions A: Basics***, Vol. 35, No. 10, (2022), 1918-1928. doi: 10.5829/IJE.2022.35.10A.11.
26. Kadam, V., Deshmukh, A. and Bhosale, S., "Hybrid beamforming for dual functioning multi-input multi-output radar using dimension reduced-baseband piecewise successive approximation", ***International Journal of Engineering, Transactions A: Basics***, Vol. 36, No. 1, (2023), 182-190. doi: 10.5829/IJE.2023.36.01A.20.
27. Madhu Krishna, K. and Naveen Kumar, P., "Improving the position accuracy of rover receiver using differential positioning in indian regional navigation satellite system", ***International Journal of Engineering, Transactions C: Aspects***, Vol. 36, No. 3, (2023), 497-504. doi: 0.5829/IJE.2023.36.03C.09.
28. Reigber, A. and Moreira, A., "First demonstration of airborne sar tomography using multibaseline l-band data", ***IEEE Transactions on Geoscience and Remote Sensing***, Vol. 38, No. 5, (2000), 2142-2152.
29. Moreira, A., Prats-Iraola, P., Younis, M., Krieger, G., Hajnsek, I. and Papathanassiou, K.P., "A tutorial on synthetic aperture radar", ***IEEE Geoscience and Remote Sensing Magazine***, Vol. 1, No. 1, (2013), 6-43. doi: 10.1109/MGRS.2013.2248301.

Persian Abstract

چکیده

این مقاله یک رویکرد مهندسی جدید برای شناسایی اهداف با استفاده از رادارهای چند استاتیکی پیشنهاد می‌کند. زاویه دیافراگم و احتمال هشدار کاذب تشخیص را در نظر می گیرد که امکان بهبود عملکرد استقرار سیستم رادار را فراهم می کند. این روش پیشنهادی بر روی سه حالت توموگرافی رادارهای چند استاتیکی آزمایش می‌شود: خروجی چندگانه ورودی (SIMO)، خروجی چندگانه ورودی (MIMO)، و رادار دیافراگم مصنوعی .(SAR) در این کار، یک روش محاسبه و تخمین برای پارامترها (حسگر فاصله و زاویه شیب خط مبنا) با استفاده از استقرار سیستم رادار بر اساس آرایش‌های هندسی توسعه داده شده است. استفاده از این پارامترها، برآورد شده توسط روش پیشنهادی، و استفاده از آنها برای محاسبه وضوح توموگرافی، نزدیکترین محل ابهام، و از دست دادن اسکن که عملکرد استقرار رادار است. نتایج نشان می‌دهد که فاصله بین سنسورها از ۴۰ تا ۷۰ درصد با افزایش زاویه دیافراگم از ۱۵ درجه به ۳۰ درجه و گام تغییرات $[\![10]\!]^{8}(-3)$ در احتمال تشخیص کاذب تغییر می‌کند. طول استقرار سیستم راداری نیز ٦.٦٦ درصد کاهش یافته است. این رویکرد قابلیت های تمایز اهداف را در یک سیستم رادار چند استاتیکی بهبود می بخشد و امکان کاهش هزینه های استقرار را فراهم می کند.